(24)

SUMMARY OF ROTOR-BLADE VIBRATORY-LOAD STUDIES

By LeRoy H. Ludi

Langley Research Center

The rotor-powered aircraft is directly associated with fatigue since the rotor is subjected to alternating aerodynamic loadings during all flight regimes. These alternating loadings on the rotor can produce periodic loads on the various components of the helicopter which could severely limit the service life of these components because of fatigue. In order to enable prediction of a satisfactory service life for these components, it is necessary to know which conditions result in the most severe periodic loads so that they may be investigated during prototype testing. Examples of conditions which require investigation are as follows:

(1) Level flight throughout speed range
(2) Retreating-blade stall
(3) Landing approaches
(4) Partial-power descents
(5) Droop-stop pounding on the ground
(6) Atmospheric turbulence
(7) Moderate maneuvers
(8) Transition
(9) High-speed level turns
(10) Pull-outs from autorotation
(11) Autorotation at high forward speed with high rotor speed

The loads in these conditions in combination with the amount of time spent in the conditions are the basic factors in a rational determination of the fatigue life of a structure. In order to determine experimentally the information on the relative severity of the periodic moments encountered by a rotor blade during the conditions listed previously, a program utilizing the helicopter shown in figure 1, equipped with strain gages at 14 percent and 40 percent of the radius on one of the blades, was undertaken. These locations were chosen to give a maximum amount of information on the blade moments and were considered adequate for this investigation even though stress surveys usually involve more locations. The results are of general interest in that the flight conditions, which resulted in the most severe rotor-blade loads are defined. The conditions numbered 1 to 5 in the previous list were found to produce the more severe blade loads and will be discussed in more detail. Additional information on all the conditions listed previously can be obtained from references 1 to 4.

Before going into the results of the rotor-blade vibratory-load studies, it is interesting to see how much time a helicopter actually spends in its various operating airspeed ranges under continued operational use as shown in figure 2. The information in this figure is a result of a continuing study of operating experiences being obtained from both civil and military operations. Published information on surveys of helicopter operating conditions is contained in references 5 to 8. Figure 2 shows the percent of total time spent in the various speed regimes as a function of the ratio of forward velocity V to the maximum forward velocity V_{MAX}. The maximum forward velocity is determined from the pilot's handbook for the particular configuration. The distribution represents the complete flight profile of climb, en route, and descent for a helicopter in both a civil application as shown by the solid line and a military application as shown by the dashed line. As can be seen from the figure, the airmail operation tends to concentrate the major percentage of total time at speeds beyond 65 percent of V_{MAX}. The military operation, in this case pilot training, tends to shift the major percentage of total time toward the lower speeds. In fact, the military operation did not spend any time above 87 percent of the maximum speed. These results show that the entire speed spectrum must be checked for large moments, particularly when the helicopter has a dual mission. The high-speed end of the spectrum, where the large percentage of time spent and the expected increased moments are combined, is extremely important in fatigue-life calculations.

In order to illustrate how the rotor-blade vibratory moments are affected by forward speed, figure 3 shows the variation of measured vibratory moments as a function of the ratio of forward velocity to maximum forward velocity. The measured vibratory moments at any speed M are divided by the measured vibratory moments at cruise speed M_{CRUISE}. Cruise speed for this helicopter is 60 percent of its maximum velocity, and the vibratory moments at cruise speed are used as a reference for most of the following figures. The moments shown in figure 3 are flapwise bending moments at 40 percent and 14 percent of the blade radius and torsional moments at 14 percent of the blade radius. The torsional moments on the blade, while not as critical as bending moments in determining the fatigue life of the blade itself, are of prime importance in control-system design. In figures 3 to 8, amplitude and revolution or cycle are defined as shown in the small inset in figure 3. It can be seen that the trends for all three moments are similar. The buildup in moment value at 25 percent of the maximum forward speed is caused by the transition region, which is the region between hovering and the speed for minimum power and is characterized by a change in airflow through the rotor. As the speed increases above 70 percent of V_{MAX}, retreating-blade stall becomes

more responsible for the increased moments. At 95 percent of V_{MAX}, the highest speed achieved during this investigation, the flapwise bending moments at 40 percent of the blade radius had increased to twice the cruise value while the torsional moments at 14 percent of the blade radius had increased to $3\frac{1}{4}$ times the cruise value. The trends indicate that the use of turbine engines and the resultant higher ratio of cruise speed to maximum forward speed will produce very high moments that must be accounted for during fatigue-life calculations.

An additional problem which arises as a result of high-speed flight is increased periodic control loads in high-performance prototype helicopters. The increased periodic control loads, a result of increased torsional moments caused by retreating-blade stall, have seriously restricted the normal operating limits of these prototypes. The effect of stall on the torsional moments is illustrated in figure 4. In this figure, the torsional moments at the various forward speeds M are divided by the torsional moment at the speed which first produced a retreating tip angle of 12° M_{STALL} and plotted against increasing forward speed. The open symbols represent unstalled conditions, and the solid symbols represent stalled conditions. It can be seen that the moments increase at a fairly shallow rate until the retreating tip angle of attack exceeds the stall angle; then, they increase rapidly. Moderate penetration into stall results in ratios that are still fairly small while extreme penetration results in ratios of almost 3. These increased vibratory torsional moments illustrate the fact that careful consideration must also be given to control-system loads during high-speed flight in order to avoid operating limitations.

At the other end of the speed spectrum, there are flight conditions which were found to produce severe periodic rotor-blade moments that would be of interest in the design of the various rotorcraft components. Landing approaches and partial-power descents at zero or low forward speeds resulted in moments that were the highest encountered during the investigation. The maximum vibratory moments experienced by the rotor blade during a landing approach are shown in figure 5. In this figure, the inboard blade moments M are divided by the cruise moment M_{CRUISE} and plotted as a function of the forward speed ratio during the approach. Since the results obtained during the landing-approach tests are not readily repeatable, the moments in this figure represent the maximum values obtained during the investigation. Since there is scatter in this type of maneuver, the amount of scatter in the area of most interest is indicated by the shaded area and is discussed in detail later. In general, figure 5 shows that flapwise bending moments as high as 5.75 times the cruise moments are encountered during

the approach. These increased moments in the landing approach are believed to be caused by a change in the airflow similar to that which occurs during the transition region.

The effect of partial-power descents on the maximum vibratory moments encountered by a rotor blade is shown in figure 6. In this figure, the ratio of the inboard flapwise moments is shown as a function of the rate of descent, for two values of forward speed (0 and 28 knots). Since the moments at a particular rate of descent also are not readily repeatable, the moments plotted in the figure represent the maximum moments encountered in the various descents. As in figure 5, the amount of scatter during the partial-power vertical descents is shown by the shaded area. Figure 6 shows that inboard moments 6.8 times the cruise moments are obtained during partial-power descents at zero forward speed. Because of the random character of the flow during the vertical descents, control was generally poor and required large movements of the controls to maintain steady conditions. As forward speed is increased to 28 knots, the moments peak at a lower rate of descent and reach a lower numerical value than those encountered in vertical descents. At the higher forward speed, control is generally improved and smaller control movements are needed to hold steady conditions. The partial-power vertical descents were found to produce the highest vibratory moments of all the conditions investigated.

Since the moments encountered during partial-power descents have a random character, the degree of conservatism involved in using the maximum moments during a partial-power vertical descent, with the assumption that the maximum moments occurred during the entire time for a fatigue-life determination, was considered. An indication of the random nature of the moments encountered during a partial-power vertical descent is given by the distribution shown in figure 7. In this figure, the ratio of the inboard bending moments is plotted as a function of the percent of total cycles in the various bending-moment ranges. Figure 7 shows that the maximum moments shown in figure 6 occur only during 1 percent of the cycles and, therefore, might be too conservative if used exclusively. Furthermore, other conditions such as high-speed flight, where the maximum moments might be above the endurance limit and occur during a larger percentage of time than the maximums in partial-power descents, must not be neglected in any rotor-blade finite life assessment.

In addition to the flight conditions investigated, static droop-stop pounding, where the blade impinges on a mechanical stop due to flapping during rotor operation on the ground, also produced some additional moments which were of interest. Static droop-stop pounding, even though artificially produced for these tests, can inadvertently occur during rotor operation on the ground in strong, gusty winds or in ground

taxiing. In fact, some cases of droop-stop pounding in the air have been reported. The potential ability to produce droop-stop pounding moments that are higher than maximum flight moments, if the pounding is allowed to progress, is illustrated in figure 8. Here the inboard flapwise moments during droop-stop pounding M are divided by the maximum flight moments $M_{FLIGHT,MAX}$ (in this case, those encountered in partial-power vertical descent) and plotted as a function of the change in longitudinal cyclic pitch $\Delta B_{1,s}$. The cyclic pitch at which droop-stop pounding first occurs is used as a reference. In general, the figure shows that the moments increase linearly with cyclic control; therefore, the moments would also increase with increasing flapping angle. This trend indicates that if the design and the operating circumstances should produce large down flapping, such as fuselage clearance often allows, very high moments will result. Even though the moments during droop-stop pounding occur at a low frequency, they can become very important from a fatigue standpoint if the magnitude of these moments follows the trend shown in the figure. The moments in the figure are felt to be an indication of the rate of increase of moment with control displacement if droop-stop pounding is inadvertently permitted, at least for a blade with uniform spar and uniform mass.

Utilization of the moments illustrated in the figures and the moments encountered during the other flight conditions investigated, in conjunction with the results of helicopter operating surveys which illustrate the amount of time spent in various flight conditions, permitted rough sample fatigue-life calculations to be made for the rotor blade. One calculation, utilizing just two of the flight conditions that produced the highest moments, was made. The fact that these moments occur during the entire time in this flight condition was assumed. The blade fatigue life under these conditions was approximately 775 hours. A second calculation, utilizing all the flight conditions that produced moments above the endurance limit and more accurate distributions of the times spent during these flight conditions, was made. The blade fatigue life under these conditions was approximately 1,510 hours. These results illustrate the necessity for an accurate evaluation of the number of flight conditions which result in the most severe periodic loads and of the time spent in each condition to be used in a fatigue-life determination for the blade in order to provide a safe blade life without undue penalties.

The results of the rotor-blade vibratory-load study indicate that severe rotor-blade loads can be expected to occur during high-speed level flight, landing approaches, partial-power descents, and droop-stop pounding during rotor operation on the ground. In addition, retreating-blade stall can cause increased torsional moments which cause increased control loads. In the future design of rotorcraft, these severe rotor-blade loads must be accurately accounted for in component fatigue-life

determinations so that undue limitations will not seriously restrict the operational usage of the rotorcraft.

REFERENCES

1. Ludi, LeRoy H.: Flight Investigation of Effects of Atmospheric Turbulence and Moderate Maneuvers on Bending and Torsional Moments Encountered by a Helicopter Rotor Blade. NACA TN 4203, 1958.

2. Ludi, LeRoy H.: Flight Investigation of Effects of Retreating-Blade Stall on Bending and Torsional Moments Encountered by a Helicopter Rotor Blade. NACA TN 4254, 1958.

3. Ludi, LeRoy H.: Flight Investigation of Effects of Transition, Landing Approaches, Partial-Power Vertical Descents, and Droop-Stop Pounding on the Bending and Torsional Moments Encountered by a Helicopter Rotor Blade. NASA MEMO 5-7-59L, 1959.

4. Ludi, LeRoy H.: Flight Investigation of Effects of Additional Selected Operating Conditions on the Bending and Torsional Moments Encountered by a Helicopter Rotor Blade. (Prospective NASA Paper.)

5. Crim, Almer D., and Hazen, Marlin E.: Normal Accelerations and Operating Conditions Encountered by a Helicopter in Air-Mail Operations. NACA TN 2714, 1952.

6. Hazen, Marlin E.: A Study of Normal Accelerations and Operating Conditions Experienced by Helicopters in Commercial and Military Operations. NACA TN 3434, 1955.

7. Connor, Andrew B., and Ludi, LeRoy H.: A Summary of Operating Conditions Experienced by Two Helicopters in a Commercial and a Military Operation. NASA TN D-251, 1960.

8. Connor, Andrew B.: A Summary of Operating Conditions Experienced by Three Military Helicopters and a Mountain-Based Commercial Helicopter. NASA TN D-432, 1960.

TEST HELICOPTER

Figure 1

DISTRIBUTION OF OPERATING AIRSPEED

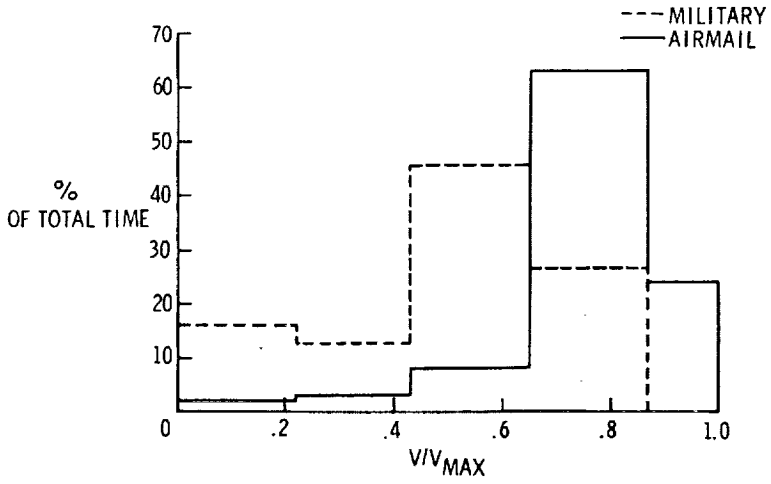

Figure 2

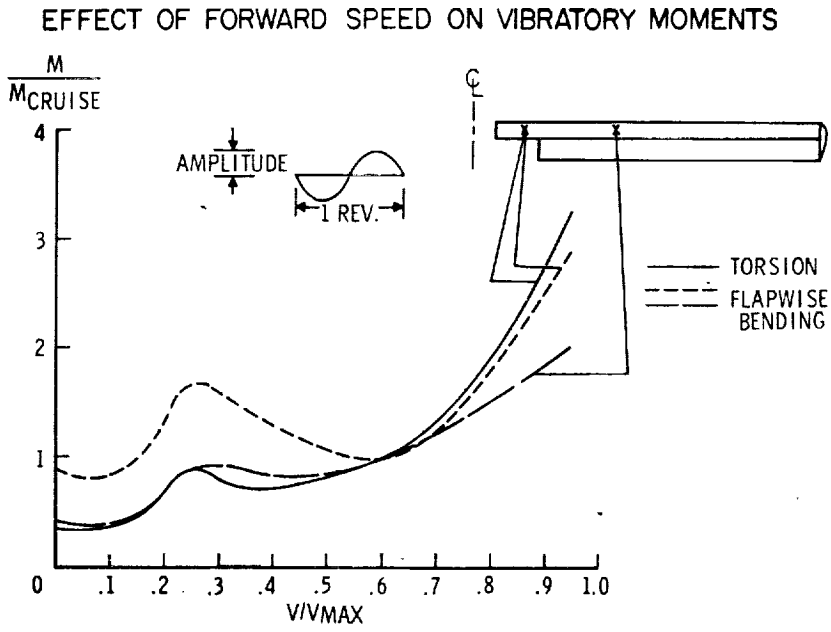

Figure 3

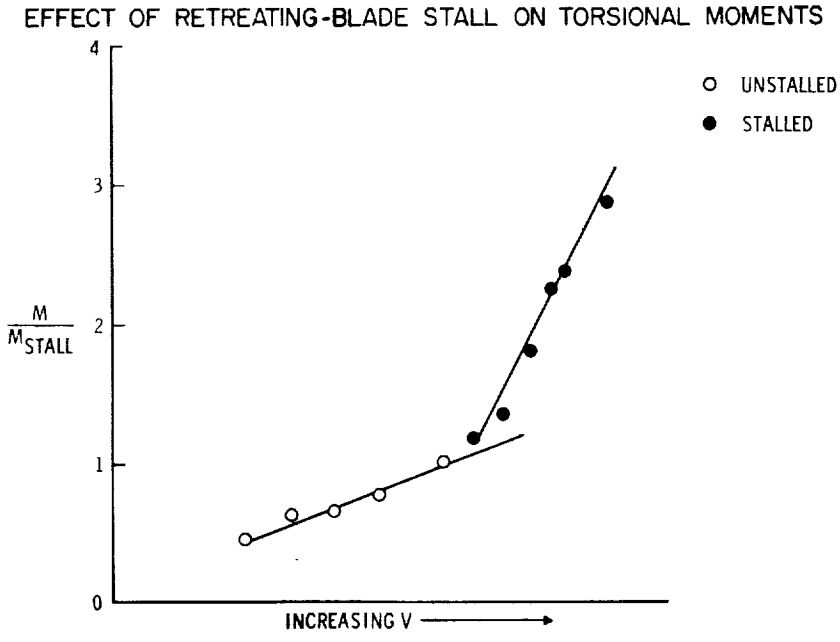

Figure 4

INBOARD FLAPWISE MOMENTS DURING LANDING APPROACH

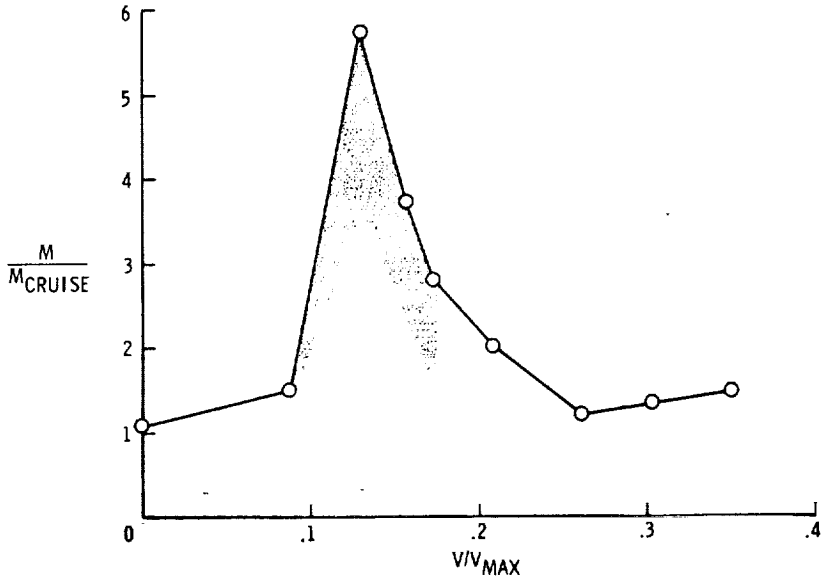

Figure 5

INBOARD FLAPWISE MOMENTS DURING PARTIAL-POWER DESCENTS

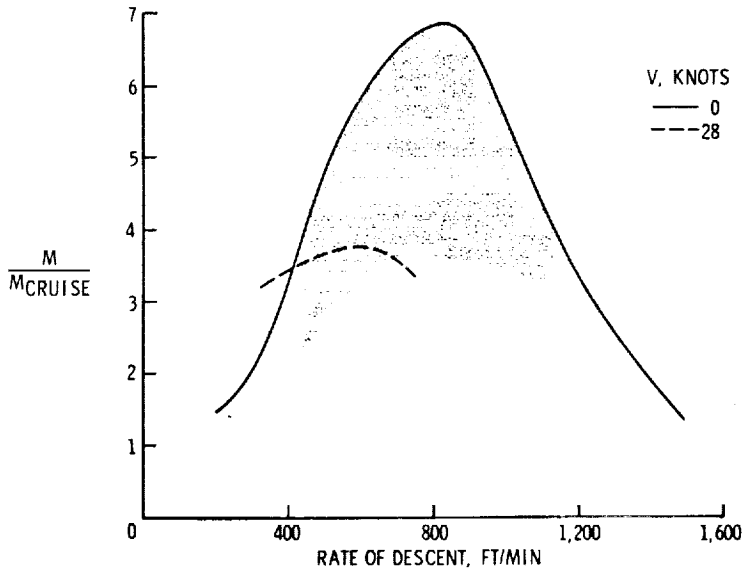

Figure 6

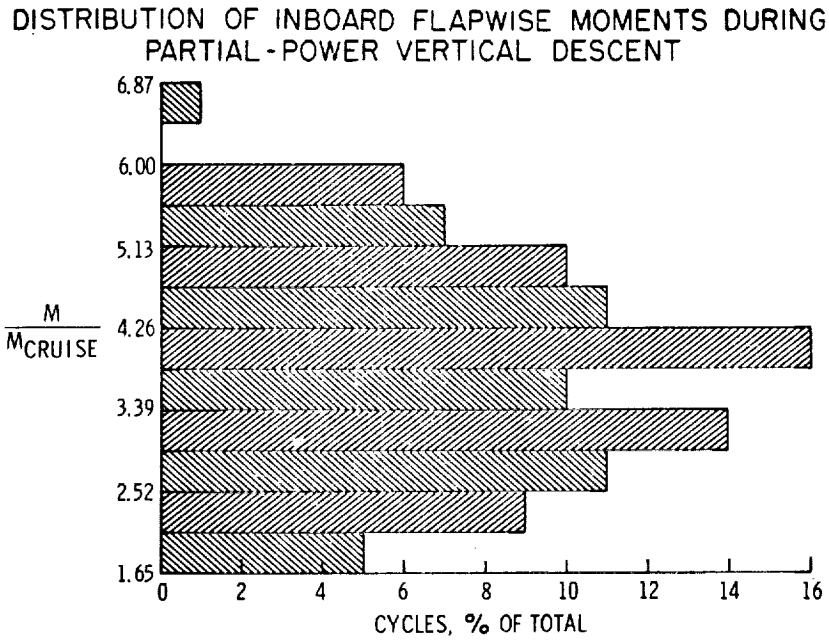

Figure 7

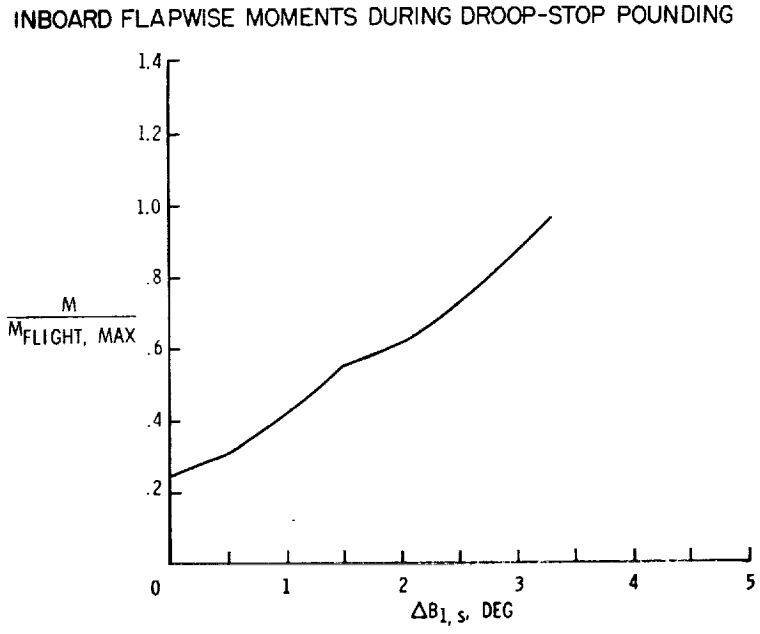

Figure 8